Correlation of the O-Intermediate Rate with the pK_a of Asp-75 in the Dark, the Counterion of the Schiff Base of *Pharaonis* Phoborhodopsin (Sensory Rhodopsin II)

Masayuki Iwamoto,*† Yuki Sudo,† Kazumi Shimono,† Tsunehisa Araiso,* and Naoki Kamo*
*Laboratory of Biomolecular Systems, Center for Advanced Science and Technology; and †Laboratory of Biophysical Chemistry, Graduate School of Pharmaceutical Sciences, Hokkaido University, Sapporo, Japan

ABSTRACT *Pharaonis* phoborhodopsin (*p*pR), also called *pharaonis* sensory rhodopsin II, NpSRII, is a photoreceptor of negative phototaxis in *Natronomonas (Natronobacterium) pharaonis*. The photocycle rate of *p*pR is slow compared to that of bacteriorhodopsin, despite the similarity in their x-ray structures. The decreased rate of the photocycle of *p*pR is a result of the longer lifetime of later photo-intermediates such as M- (ppR$_M$) and O-intermediates (ppR$_O$). In this study, mutants were prepared in which mutated residues were located on the extracellular surface (P182, P183, and V194) and near the Schiff base (T204) including single, triple (P182S/P183E/V194T), and quadruple mutants. The decay of ppR$_O$ of the triple mutant was accelerated ~20-times from 690 ms for the wild-type to 36 ms. Additional mutation resulting in a triple mutant at the 204th position such as T204C or T204S further decreased the decay half-time to 6.6 or 8 ms, almost equal to that of bacteriorhodopsin. The decay half-times of the ppR$_O$ of mutants (11 species) and those of the wild-type were well-correlated with the pK_a value of Asp-75 in the dark for the respective mutants as spectroscopically estimated, although there are some exceptions. The implications of these observations are discussed in detail.

INTRODUCTION

Phoborhodopsin (pR, also called sensory rhodopsin II, or SRII) is a member of an archaeal rhodopsin family and acts as a sensor of negative phototaxis (Takahashi et al., 1985). Recently, *pharaonis* phoborhodopsin (*p*pR, also called *pharaonis* sensory rhodopsin II, or NpSRII), from *Natronomonas (Natronobacterium) pharaonis* was extensively investigated instead of pR due to its high stability (Hirayama et al., 1992; Chizhov et al., 1998; Pebay-Peyroula et al., 2002; Scharf et al., 1992; Spudich and Luecke, 2002; Iwamoto et al., 2003b). This pigment protein has seven transmembrane helices into which a chromophore, all-*trans* retinal, binds to a specific lysine residue on the G-helix to form a protonated Schiff base. This type of feature is common among other archaeal rhodopsins such as bacteriorhodopsin (BR) (Haupts et al., 1999; Luecke and Lanyi, 2003; Oesterhelt and Stoeckenius, 1971), halorhodopsin (hR) (Essen, 2002; Varo, 2000; Matsuno-Yagi and Mukohata, 1977), and sensory rhodopsin (sR or sRI) (Bogomolni and Spudich, 1982; Hoff et al., 1997), which constitute an outward light-driven proton pump, inward light-driven Cl^- pump, and phototaxis sensor other than for phoborhodopsin (pR) or sensory rhodopsin II (SRII), respectively. Many investigations on the structure and function of BR have been carried out, and thus BR is one of the best-understood membrane proteins.

The functional expression of *p*pR in *Escherichia coli* (Shimono et al., 1997) had been achieved, affording the expression of a large amount of proteins and therefore permitting its detailed characterization. The crystal structure of *p*pR (Gordeliy et al., 2002; Luecke et al., 2001; Royant et al., 2001) has almost the same three-dimensional structure as that of BR, implying that the functional differences in these two proteins originate from differences in their amino acid side chains.

The illumination of archaeal rhodopsins elicits a cyclic and linear photoreaction called photocycling, during which these pigments function. The photocycle intermediates in *p*pR are denoted as K, L, M, N, and O, and are analogous to those of BR. The presence of an N-intermediate has been suggested by multi-exponential global analysis of the photocycle of *p*pR (Chizhov et al., 1998), but its nature is not well understood. Fourier transform infrared studies (FTIR; Furutani et al., 2002; Iwamoto et al., 2003a) revealed that *p*pR does not possess an N-like protein structure characteristic of the N-intermediate of BR. Upon formation of the M-intermediate of BR (BR_M), primary proton transfer from the protonated Schiff base to its counterion Asp-85^{BR} occurs followed by proton release from the proton-releasing group (PRG) to the extracellular surface. A subsequent

Submitted May 5, 2004, and accepted for publication September 9, 2004.

Address reprint requests to Masayuki Iwamoto, Division of Molecular Physiology and Biophysics, Dept. of Morphological and Functional Biomedical Science, Faculty of Medical Science, University of Fukui, Matsuoka 910-1193, Japan. Tel.: 81-776-61-8306; Fax: 81-776-61-8101; E-mail: zz04004@fmsrsa.fukui-med.ac.jp.

Abbreviations used: BR, light-adapted bacteriorhodopsin; CAPS, 3-(cyclohexyl-amino-9-1-propanesulfonic acid; CHES, 2-(*n*-cyclohexyl-amino)ethanesulfonic acid; DM, *n*-dodecyl-β-D-maltoside; HEPES, *n*-2-hydroxyethylpiperazine-*n*′-ethanesulfonic acid; MES, 2-(*n*-morpholino)ethanesulfonic acid; MOPS, morpholinopropane-sulfonic acid; *p*pR, *pharaonis* phoborhodopsin (sensory rhodopsin II); ppR$_M$, M-intermediate of *p*pR; ppR$_O$, O-intermediate of *p*pR; PC, L-α-phosphatidylcholine from *egg*.

0006-3495/05/02/1215/09 $2.00

doi: 10.1529/biophysj.104.045583

cascade of proton movements is then induced, consisting of uptake from the cytoplasmic surface by the deprotonated Schiff base via Asp-96^{BR} and transfer from Asp-85 to deprotonated PRG as the final step of the photocycle. These proton transfers therefore result in outward proton pumping. Upon ppR$_M$-formation, ppR also undergoes proton transfer from the protonated Schiff base to its counterion Asp-75^{ppR} (Engelhard et al., 1996; Furutani et al., 2002), followed by proton release from Asp-193, which corresponds to Asp-204^{BR} (Iwamoto et al., 2004). Proton uptake subsequently occurs, leading to protonation of the deprotonated Schiff base. Therefore, ppR can pump protons from the cytoplasmic side to the extracellular side, although its activity is weak (Schmies et al., 2000; Sudo et al., 2001b).

The photocycling rate is different between BR and ppR; the M- and O-intermediates of BR (BR$_M$ and BR$_O$) decay within 10 ms whereas it takes several hundred milliseconds to several seconds for the M- and O-like intermediates of ppR (ppR$_M$ and ppR$_O$) to decay. The difference in the photocycling rates is related to the function of these proteins. For efficient ion pumping, a fast photocycle is required, whereas the slowness of the ppR photocycle is relevant to its function during signal transduction. Phototaxis is achieved by modulating cell swimming behavior through signal transduction from light-activated ppR to a cognate transducer protein, *pharaonis* halobacterial transducer II (pHtrII). The intermediates of ppR$_M$ and ppR$_O$ are the signaling states (Yan et al., 1991; Wegener et al., 2000), and their long lifetimes may be required for sufficient signal transduction to the transducer protein.

The molecular origin of this slow photocycling and the residues that contribute to this are unknown. The slowness of ppR$_M$-decay originates from retarded reprotonation of the deprotonated Schiff base through a hydrophobic cytoplasmic channel (CP) because of the lack of dissociable amino acid residues corresponding to Asp-96^{BR} in BR. Replacement of Phe-86^{ppR} with Asp together with the replacement of Leu-40 with Thr accelerates ppR$_M$-decay (Iwamoto et al., 1999; Klare et al., 2002). On the other hand, the decay time constant of ppR$_O$ is ~3–4 s^{-1}, and only one study by Klare et al. (2002) has been carried out to investigate the cause of this slow decay on a molecular basis. Analogous to BR, ppR$_O$-decay coincides with proton transfer from protonated Asp-75 to PRG at the extracellular surface through an extracellular proton conduction channel. A comparison of the amino acid alignment of BR and ppR (Seidel et al., 1995) in an extracellular channel (EC) suggests a higher hydrophobicity for ppR than BR. Here, the hydrophilic residues of Ser-193^{BR}, Glu-194^{BR} and Thr-205^{BR} in BR are replaced by Pro-182^{ppR}, Pro-183^{ppR}, and Val-194^{ppR} in ppR, respectively, but the negative charge of Glu-204^{BR} is conserved as Asp-193^{ppR}. In addition to these three amino acid residues, Klare et al. (2002) noted that Thr-204^{ppR} influences ppR$_O$-decay. In this study, we prepared various single-, triple-, and quadruple-point mutants of these four residues. Replacement accelerated the decay and decay half-time of ppR$_O$, which was positively well-correlated with the pK$_a$ of Asp-75 in the dark. The implications of this observation are discussed in detail.

MATERIALS AND METHODS

Sample preparation

The expression and purification of histidine-tagged recombinant ppR and its mutants were prepared as previously described (Kandori et al., 2001a; Sudo et al., 2001a). Briefly, ppR and its mutant proteins possessing a histidine tag at the C-terminus were expressed in *Escherichia coli*, solubilized with 1.5% *n*-dodecyl-β-D-maltoside (DM) and purified with an Ni-column. The purified sample was then mixed with L-α-phosphatidylcholine (PC) followed by dialysis in the presence of Bio-Beads (Bio-Rad, Hercules, CA) to remove DM. The molecular ratio of the protein to PC was 1:50.

Flash photolysis spectroscopy

The apparatus and procedure used were the same as that previously described (Miyazaki et al., 1992). The PC-reconstituted samples were washed three times and suspended in a buffer containing 400 mM NaCl and six-mixed buffer (citric acid, MES, HEPES, MOPS, CHES, and CAPS at 10 mM each), which has the advantage of equal buffer capacities at any pH. The pH of the suspension was adjusted to 6.0, and the temperature was kept at 20°C by circulating temperature-regulated water inside a sample cell jacket. Analysis was performed according to Miyazaki's method (1992) to obtain the decay half-time of the intermediate.

Visible absorption spectroscopy

Absorption spectra were taken using a Model V-560 spectrophotometer (Jasco, Tokyo, Japan). The PC-reconstituted samples were washed three times and suspended in a buffer containing 133 mM Na_2SO_4 and six-mixed buffer, where the temperature was kept at 20°C by circulating temperature-regulated water inside a sample cell jacket. The pH titration of Asp-75 started at 7.0 to a more acidic pH by the addition of concentrated H_2SO_4, and the absorption spectra at each respective pH was measured. Accurate estimation of the O-decay rate sometimes required the presence of azide (see Table 1), and for these cases the pK$_a$ of Asp-75 of the ppR mutants was estimated in the presence of azide with the same concentration as that used for the O-decay estimation.

RESULTS

Mutations of amino acid residues in the extracellular proton conduction channel and its effect on the decay rates of late photointermediates

ppR has a relatively hydrophobic extracellular proton conduction channel (EC) compared to BR; Ser-193, Glu-194, and Thr-205 in BR are replaced by the hydrophobic residues Pro-182, Pro-183, and Val-194, respectively (Fig. 1 *A*). Then, single mutated ppR pigments were prepared in which the amino acid residue in ppR described above was replaced by the corresponding residue in BR. Flash-photolysis data at selective wavelengths for these mutants

TABLE 1 Decay half-times for the late photo-intermediates and pK_a of Asp-75 in wild-type and *pp*R mutants

	M-decay (ms)	O-decay (ms)	pK_a of Asp-75
Wild-type	890	690	3.4 (±0.06)
+ azide*	8.8	150	3.0 (±0.10)
P182S	870	1000	3.5 (±0.04)
P183E	430	99	2.7 (±0.06)
V194T	430	180	3.4 (±0.10)
S/E/T†	150	36	3.0 (±0.06)
T204A	3700	ND	3.2 (±0.08)
+ azide*	66	97	2.6 (±0.14)
T204C	1200	ND	3.3 (±0.07)
+ azide*	20	35	3.1 (±0.12)
T204S	1800	ND	3.2 (±0.07)
+ azide*	26	43	2.9 (±0.16)
T204V	1200	5800	3.7 (±0.10)
+ azide*	100	7700	3.8 (±0.15)
S/E/T/A‡	520	ND	3.0 (±0.08)
+ azide*	9.8	31	2.9 (±0.17)
S/E/T/C§	230	ND	2.8 (±0.05)
+ azide*	19	6.6	2.7 (±0.08)
S/E/T/S‖	280	ND	2.8 (±0.05)
+ azide*	20	8.0	2.7 (±0.06)

The experimental conditions are described in Materials and Methods. *ND* means *not determined*; determination of the decay half-time of pR_O was difficult because of the slow decay of the preceding pR_M. For this case, azide was added to accelerate the pR_M-decay. See text for details.
*The azide concentration was 50 mM.
†S/E/T means the triple mutant P182E/P183E/V194T.
‡S/E/T/A, §S/E/T/C, and ‖S/E/T/S indicate quadruple mutants, where S/E/T and an additional mutation at the 204th position (Thr) was performed by replacing Ala, Cys, and Ser, respectively.

are shown in Fig. 2, and the decay half-time values of the M- and O-intermediates are listed in Table 1. The decay half-time of pR_M of all single mutants essentially did not change from that of the wild-type. On the other hand, the decay of pR_O was accelerated approximately seven- and fourfold for P183E and V194T, respectively, whereas for P182S little deceleration was observed.

Next, we prepared the triple mutant P182S/P183E/V194T (abbreviated as S/E/T), which had amino acid residues similar to the EC of BR. The pR_O-decay half-time of this mutant decreased to 36 ms (i.e., ~20-fold decrease), which was still longer than that of BR at 5 ms. The pR_M-decay of the triple mutant was also accelerated, but the degree of acceleration was small compared with pR_O. These results suggest that mutation of amino acid residues at EC affects the decay of pR_O rather than pR_M.

Mutation at the 204th position of *pp*R and its effect on the decay rates of late photo-intermediates

One of the characteristic differences in amino acid alignment around the Schiff base-counterion complex region occurred between *pp*R and BR is at the 204th position of *pp*R (215th position of BR), Thr-204 in *pp*R, and Ala-215 in BR (Seidel et al., 1995). The Thr-204 of *pp*R was replaced by other residues, and the decay rates of the late photo-intermediates were then assayed (see Fig. 3). For all mutants, the pR_M decay was so slow that the estimation of the pR_O decay rate was difficult due to its very low accumulation during photocycling, as seen for the 560-nm trace in Fig. 3, *a* and *c*. To analyze the pR_O decay of these mutants, azide was added, which remarkably accelerated pR_M-decay with essentially little effect on the pR_O-decay rate (Takao et al., 1998; Iwamoto et al., 2001, 2002b). The accelerated decay of pR_M was also observed for the present PC-reconstituted sample (Fig. 3, *b* and *d*), which enabled us to estimate the pR_O-decay rate constant of the mutants, whose results are listed in Table 1. The values listed are not necessarily equal

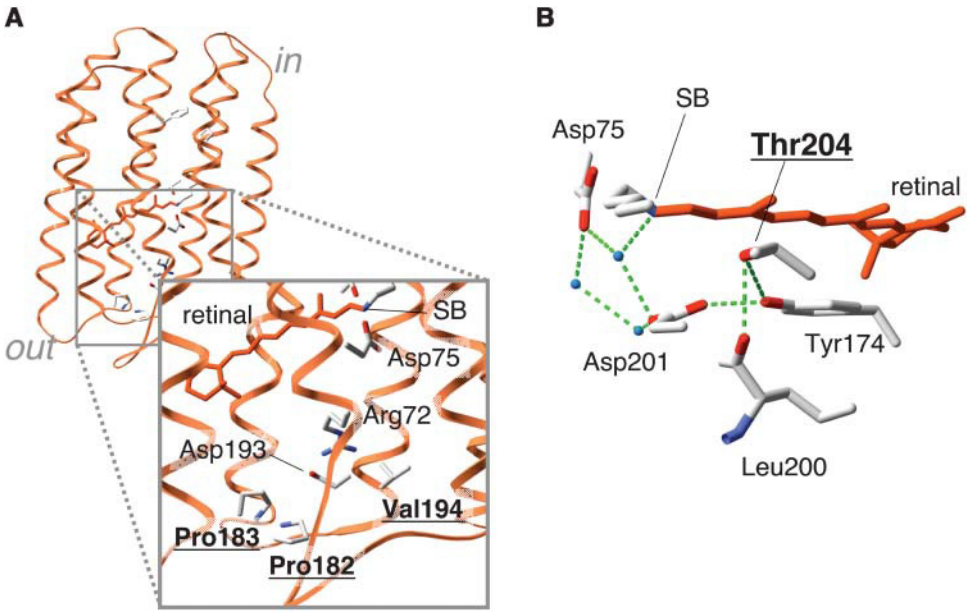

FIGURE 1 (*A*) X-ray three-dimensional crystal structure of *pp*R, where the extracellular proton conducting channel (EC) is enlarged. The amino acid residues that were replaced are shown in bold and are underlined, and other important residues are also indicated. (*B*) X-ray three-dimensional crystal structure around the region of the Schiff base and counterion of *pp*R. Water molecules are depicted as blue spheres and putative hydrogen bonds are displayed as green broken lines. These structures were obtained from the Protein Data Bank (code, 1H68).

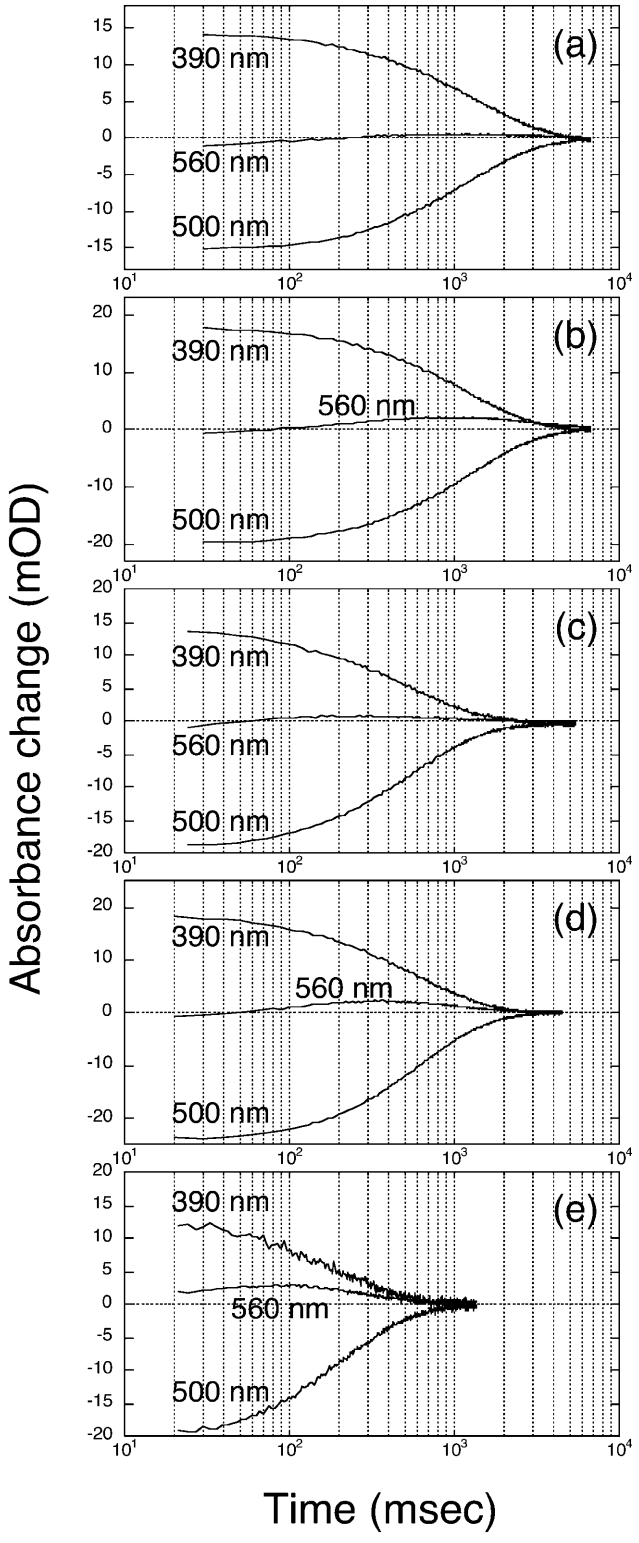

FIGURE 2 Typical flash photolysis kinetic data of three selective wavelengths for wild-type and various mutants whose extracellular surface residues were replaced. (*a*) Wild-type; (*b*) P182S; (*c*) P183E; (*d*) V194T; and (*e*) P182S/P183E/V194T. This data was obtained in the presence of 400 mM NaCl at pH 6.0 and 20°C. The absorbance changes at 390 and 560 nm were used to monitor the concentration changes of ppR$_M$ and ppR$_O$, respectively, where 500 nm is the ground state of ppR.

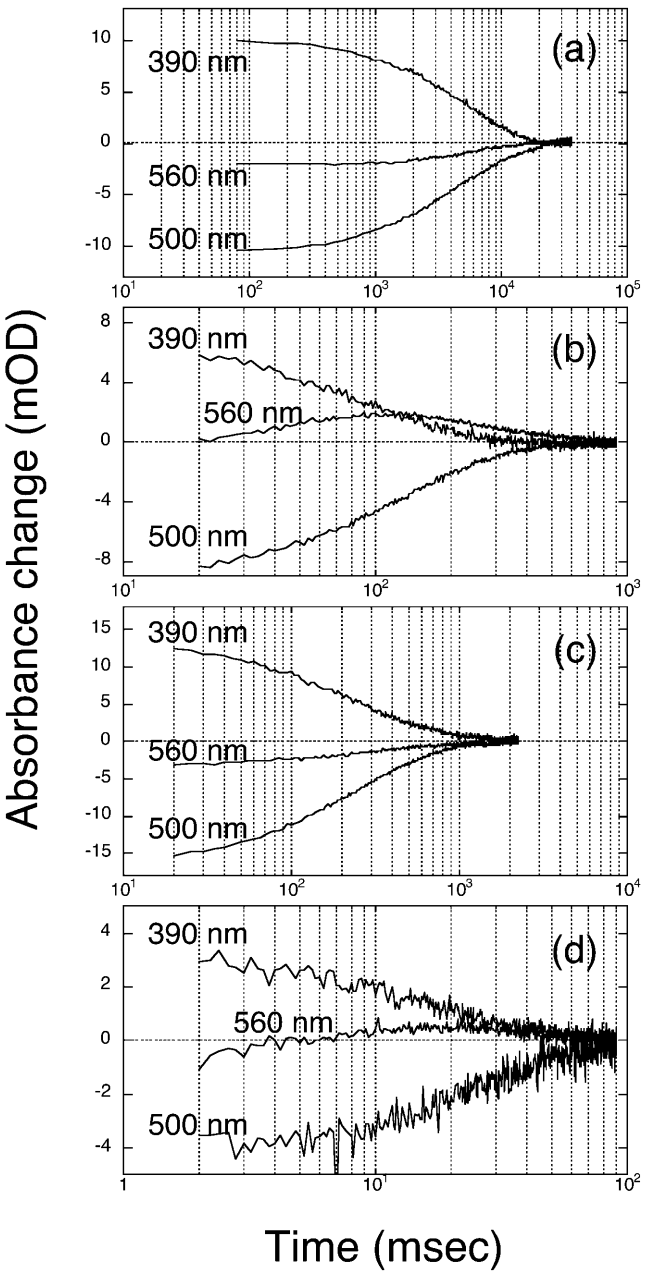

FIGURE 3 Typical flash photolysis kinetic data of three selective wavelengths. (*a*) T204A; (*b*) T204A in the presence of 50 mM azide; (*c*) P182S/P183E/V194T/T204C; and (*d*) P182S/P183E/V194T/T204C in the presence of 50 mM azide. Note the difference in the time range for *a–d*. This data was obtained in the presence of 400 mM NaCl at pH 6.0, 20°C. The absorbance changes at 390 and 560 nm were used to monitor the concentration changes of ppR$_M$ and ppR$_O$, respectively, where 500 nm is the ground state of ppR.

to those in the absence of azide because azide affects wild-type ppR$_O$-decay (Table 1), although the effect is small compared to that of ppR$_M$. As mentioned above, azide did not affect ppR$_O$-decay for the solubilized sample (Takao et al., 1998) whereas the present samples were PC-reconstituted.

Therefore, the ppR_O decay half-times of 97 (T204A), 35 (T204C), and 43 ms (T204S) were compared with 150 ms for the wild-type, which was obtained in the presence of azide. In the case of T204V, the decay half-time of ppR_O was 5800 and 7700 ms in the absence and presence of azide, respectively, and these values were larger than those for the wild-type (Table 1). The reason why the T204V mutant exhibited different behavior from the other mutants is not known; it showed a higher Asp-75 pK_a than that for the wild-type and other mutants. Thus, these results suggest that ppR_O-decay is affected by perturbation of the amino acid residue at the 204th position.

Quadruple mutation and its effect on the decay rates of late photo-intermediates

As described above, the amino acid residues at the 182nd, 183rd, 194th, and 204th positions affect the ppR_O-decay rate, and the mutant P182S/P183E/V194T (abbreviated S/E/T) showed significant accelerated ppR_O-decay. Therefore, quadruple mutants were prepared in which an additional mutation at the 204th position was added to the S/E/T mutant; they were S/E/T/A, S/E/T/C and S/E/T/S. Here, S/E/T/A signifies a quadruple mutant for T204A added to S/E/T, (i.e., P182S/P183E/V194T/T204A), and the others were accorded to the same rule. As listed in Table 1, the ppR_M-decay was faster by a factor of 2 or 4 than for the wild-type. However, the ppR_O-decay rate was difficult to assay because it was enhanced by the mutation. We therefore added azide to accelerate the ppR_M-decay, and from this estimated the ppR_O-decay rate. The results listed in Table 1 reveal a drastic acceleration of ppR_O-decay compared to the wild-type in the presence of azide. The decay half-time of 6.6 ms for S/E/T/C (Fig. 3 *d* and Table 1) was almost equal to that of BR at 5 ms. These results imply that the amino acid residues at these four positions play a significant role in proton relay during O-decay.

pK_a of Asp-75 in the ground state in the wild-type and mutants

Spectroscopic pH titration was performed to estimate the pK_a values of Asp-75 in the ground (dark) state because protonation of Asp-75 causes a red-shift at the absorption maximum. For the wild-type, Thr-204 mutant, and quadruple mutants, examinations were performed in the presence of azide with the same concentrations as those in the flash-photolysis. All pH titration experiments were carried out under Cl^--free conditions to circumvent complex interaction among Cl^-, Asp-75. and other carboxylic residues previously observed by Ikeura et al. (2004). The titration curves were analyzed using the Henderson-Hasselbalch equation with a single pK_a value, and the results are listed in the rightmost column of Table 1. The pK_a value of Asp-75 for the PC-reconstituted wild-type *pp*R was 3.4, close to that obtained for a dodecyl-maltoside (DM)-solubilized sample (Chizhov et al., 1998; Shimono et al., 2000) rather than a purple membrane-reconstituted one (Chizhov et al., 1998). We observed a variation in pK_a for Asp-75 depending on the lipid used for the reconstitution (Mizuta et al., unpublished results), especially for the electric state of the lipid. Azide affected the pK_a values of Asp-75 for almost all mutants and the wild-type, although the magnitudes of change were different. The pK_a change due to azide implies the binding of azide near Asp-75, which affects the Asp-75 environment. A similar effect on BR was reported by Coutre et al. (1995), who showed using FTIR the influence of azide on the arrangement of the intramolecular hydrogen-bonding network of water. In addition, the acceleration of ppR_M-decay implies the participation of azide as a shuttle between the Schiff base and outer medium. The pK_a value of Asp-85 of BR is 2.6, and some mutants used in the present study exhibited values close to this. For example, those of T204A, S/E/T/C, and the wild-type in the presence of azide were 2.6, 2.7, and 3.0, respectively. On the other hand, the pK_a values of T204V in the presence or absence of azide were larger than those for the wild-type at 3.8 and 3.7, respectively, and azide increased pK_a in comparison to the others. Azide increased the decay half-time of ppR_O of this mutant, and this was the only exception among the mutants examined (Table 1).

Relationship between the pK_a of Asp-75 and the decay half-times of late photo-intermediates

Fig. 4 shows plots of the decay half-time of ppR_M (Fig. 4 *A*) and that of ppR_O (Fig. 4 *B*) versus the pK_a values of Asp-75 for pK_a values in the ground (dark) state. When ppR_O-decay was estimated in the presence of azide, the pK_a of Asp-75 was also estimated with the same concentration. A good correlation was seen between the decay half-time of ppR_O and the pK_a of Asp-75 in the ground state (Fig. 4 *B*), although some points did not fall on the line such as for T204A in the presence of azide, P183E, and V194T. In Fig. 4 *A*, the data obtained in the presence of azide was deleted because the rate of ppR_M-decay under this condition was determined by the shuttle mechanism (Takao et al., 1998).

DISCUSSION

In this study, we showed that the relatively hydrophobic extracellular proton conduction channel (EC) of *pp*R compared to BR is one cause of slow ppR_O-decay, which can be concluded from the results for single Pro-182, Pro-183, or Val-194 point mutations and those for the simultaneous triple-point mutation of these residues (Fig. 2). In addition, the ppR_O-decay rate perturbation affects the amino acid residue at the 204th position (Fig. 3). The pK_a of Asp-75 in the dark exhibits a good correlation with the ppR_O

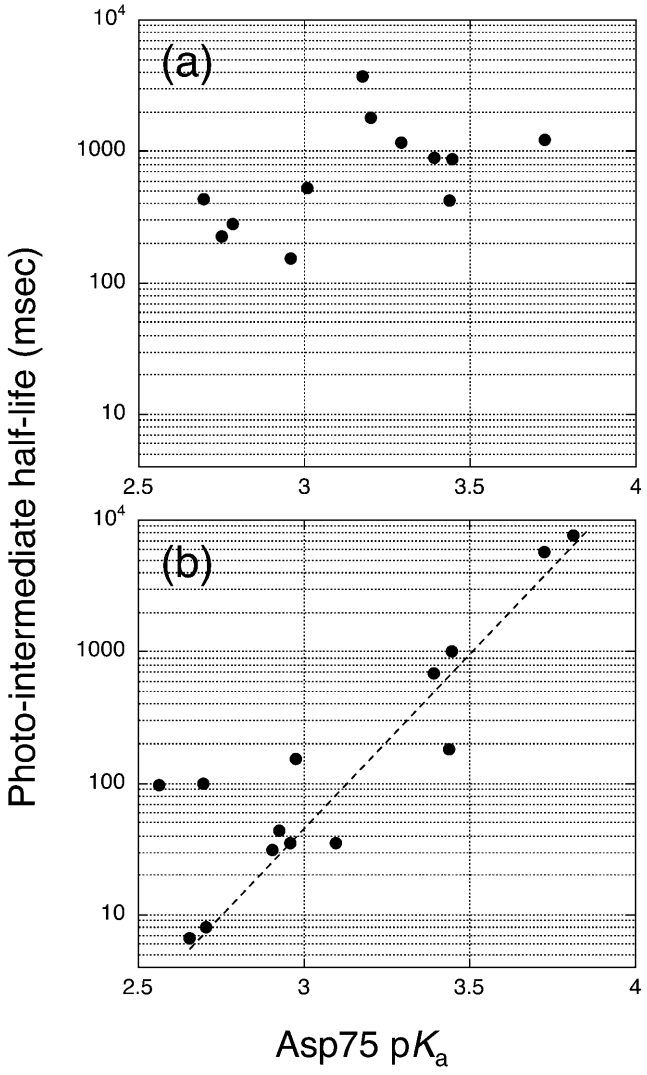

FIGURE 4 The relationship between the pK_a of Asp-75 in the ground state and the decay half-time of ppR$_M$ (*a*) and ppR$_O$ (*b*) of the wild-type and various mutants of ppR. The plotted data was derived from Table 1.

lifetime (Fig. 4 *b*) and a poor correlation with that of ppR$_M$ (Fig. 4 *a*).

From the results, we inferred the following; during O-decay, the proton released from protonated Asp-75 is transferred through the EC proton conductive channel as occurs in BR, where intraprotein transfer from Asp-85^{BR} to PRG occurs (Hessling et al., 1993; Kandori et al., 1997). This implies the existence of hydrogen-bonding pathways through EC during ppR$_O$-decay. A previous report (Iwamoto et al., 2002a) showed that the mutation of Asp-193 to Asn changes the pK_a of the Schiff base far from the 193rd position, suggesting the existence of long-range interactions through the EC in the ppR ground state.

The mutation of Thr-204 affects ppR$_O$-decay. ppR and BR possess similar environments around the Schiff base and its counterion (Asp-75^{ppR} and Asp-85^{BR}), where three water molecules exist in the region of the Schiff base and its counterion to form a pentagonal hydrogen-bonding cluster involving the counterion and the other Asp (Asp-201^{ppR} and Asp-212^{BR}). Around this region, however, is one characteristic difference between ppR and BR—the existence of Thr-204^{ppR}, with its corresponding residue being Ala-215^{BR} in BR. Klare et al. (2002) examined the effect of this residue on ppR$_O$-decay using a L40T/F86D/P183E/T204A mutant and observed an acceleration in the decay. They interpreted this to be due to a size effect: replacement with the smaller residue (Thr by Ala) facilitates the mobility of the protein upon ppR$_O$-decay. In addition, the present results showed the interaction of Thr-204 with the pentagonal hydrogen-bonding cluster, which might change the pK_a of Asp-75 (see Table 1).

As described above, the most important observation in this study was the strong correlation of the pK_a of Asp-75 with the decay half-time or decay rate of ppR$_O$, although the pK_a value was that of the ground state and there were some deviations for some mutants such as V194T, P183E, and T204A. For the ppR$_O$ decay rate of Arg-72 mutants reported by Ikeura et al. (2004), replacement of Arg-72 increases the pK_a of Asp-75 to above 4 from 3.5 for the wild-type, whereas the decay half-time of ppR$_O$ is not necessarily prolonged. R72K, whose pK_a for Asp-75 is 4.4, exhibits a longer half-time than that of the wild-type, whereas others, including R72A and R72Q, whose pK_a values for Asp-75 are 5.7 and 6.0, respectively, exhibit a shorter half-time. Therefore, one possibility is that the rule noted here may hold under the limitation that the pK_a of Asp-75 $< \sim 4$. Another possibility is that replacement of Arg-72 interrupts the hydrogen-bonding network that extends from the extracellular side to the Schiff base region, which was revealed by an analysis of the pK_a of Asp-75 and from the timing of proton release during the photocycle (Ikeura et al., 2004). Of these, the latter possibility seems most reasonable.

Mutants of BR having slow O-decay rates have been previously reported: mutations of Glu-204^{BR} (Brown et al., 1995; Richter et al., 1996), Glu-194^{BR} (Balashov et al., 1997, 1999; Dioumaev et al., 1999), and also Tyr-57^{BR} (Lanyi, 1993). Here, the mutation of Tyr-57^{BR} might alter the proton-pathway. The mutation of PRG of BR leads to a slower O-decay. In addition, the rate constant of O-decay of the wild-type BR decreases for a pK_a of 4.5, which is close to the pK_a of the PRG in the blue membrane (Balashov et al. 1999). Therefore, deprotonation of Asp-85^{BR} only occurs after deprotonation of PRG, or when PRG controls the O-decay rate, or after deprotonation of Asp-85^{BR}. This relationship was found to be enhanced by using a E194D^{BR} mutant, which showed a parallel pH-shift between the pK_a of PRG and the O-decay rate (Balashov et al., 1999), which is opposite to the experimental observations seen in this study. The mutation of Glu-204^{BR} (E204Q) greatly slows the O-decay (Brown et al., 1995; Misra et al., 1997; Balashov et al., 1999) as described above, whereas it lowers the pK_a of Asp-85^{BR} in the ground state (Richter et al., 1996). In

addition, different ppR_O-decay behavior compared to that of BR was observed. The rate constants of the ppR_O-decay (reconstituted with 50-fold lipids) at various pH were 0.9 (pH 7), 1 (pH 6), 2 (pH 5), and 6 s^{-1} (pH 4), which are in sharp contrast to that of BR, for which the rate decreases in acidic solution with a pK_a of 4.5 (Balashov et al., 1999). $E194Q^{BR}$ or $E204Q^{BR}$ mutations, which disable the PRG, slow the O-decay by a factor of 10–30 above pH 4.5 without pH-dependence. On the contrary, the O-decay rates of $D193N^{ppR}$ were 4 (pH 7), 3 s^{-1} (pH 4–6), unlike those for BR. These observations suggest that the rate-determining steps of the O-decay are different between BR and *pp*R, although the hydrogen bonding network extends from PRG to the Schiff base for both proteins. For BR, deprotonation of PRG is the rate-determining event, whereas for *pp*R deprotonation of Asp-75, the counterion of protonated Schiff base, is the rate-determining event. The molecular basis of this difference is not known, but it is most likely that the different orientation of guanidium of $Arg\text{-}72^{ppR}$ and $Arg\text{-}82^{BR}$ (Luecke et al., 2001; Royant et al., 2001; Gordeliy et al., 2002) alters the coupling strength of hydrogen bonding of EC or changes the pK_a of important residues during O-decay. As described above, $Arg\text{-}72^{ppR}$ mutants do not follow the rule shown in Fig. 4, which might be evidence of the importance of the Arg residue; the presence of the Arg-residue is necessary for the hydrogen bonding network to extend from PRG to the Schiff base, but the different orientation of its guanidium alters the coupling strength. This difference could be checked in future by the D_2O effect on the O-decay.

Another phenomenon seen in Fig. 4 *b* is the slope of the correlation line, which is larger than unity, the reason for which is not known. However, a slope larger than unity suggests the existence of positive cooperativity; deprotonation of Asp-75 might induce the proton pathway in EC. In Fig. 4, deviations from the straight relationship can be seen for some mutants, although it is unknown why this occurs. However, it is plausible that the acceleration of O-decay might originate from factors other than the pK_a of $Asp\text{-}75^{ppR}$, such as for $Tyr\text{-}57^{BR}$ as mentioned above.

Another hypothesis is the parallel nature of the pK_a of $Asp\text{-}75^{ppR}$ between the unphotolyzed state and the O-state. For BR, the pK_a of $Asp\text{-}85^{BR}$ is ~2.6 in the ground state, and increases to >11 in the BR_M-state (Brown et al. 1993). Therefore, the pK_a of $Asp\text{-}75^{ppR}$ should also change during the photocycle. Nevertheless, we assumed here that the pK_a of $Asp\text{-}75^{ppR}$ in the O-state might be proportional to that in the dark state. This is reasonable if the hydrogen bonding of unphotolyzed *pp*R is not well-organized in comparison with BR (Kandori et al., 2001b) due to the distorted pentagonal hydrogen-bonding cluster. The pK_a change in $Asp\text{-}75^{ppR}$ at the photointermediate with the disrupted pentagonal cluster might therefore be less affected by the protonated states of other residues or by the conformational change than for BR. In addition, since for BR the hydrogen bonding coupling strength in EC is strong, one cannot distinguish whether protonation of the PRG or the deprotonation of $Asp\text{-}85^{BR}$ is the driving event that initiates O-decay.

Fig. 4 *a* shows a poor correlation of pK_a with the decay half-time of ppR_M, since its half-time is regulated by the reprotonation rate of the deprotonated Schiff base, which is in turn influenced by dissociable amino acid residues in the cytoplasmic channel (Iwamoto et al., 1999; Klare et al., 2002). Although the correlation is weak, as pK_a decreases, the decay half-time of ppR_M decreases (Fig. 4 *a*). This might occur because, during ppR_M-decay, some of protons that reprotonate the Schiff base come from the extracellular (EC) as well as the cytoplasmic surfaces (Ikeura et al., 2004), and even for ppR_M-decay the pK_a of Asp-75 influences proton conduction of the EC channel presumably due to the hydrogen bonding network.

A prolonged decay half-time of late photo-intermediates such as M- and O-intermediates is important for signal transduction to *p*HtrII, a cognate transducer protein of *pp*R, because these intermediates occur in the signaling state (Yan et al., 1991; Wegener et al., 2000). On the other hand, a rapid photocycle is required for ion-pumping archaeal rhodopsins. Thus, archaeal rhodopsins control their photocycling rates depending on their function. Proton transfer reactions, which regulate the decay rate of photo-intermediates during the photocycle, might be one crucial factor responsible for the physiological functions of archaeal rhodopsins, for which the rate of reaction is controlled by a few amino acid residues.

This work was supported by Research Fellowships from the Japan Society for the Promotion of Science for Young Scientists to M.I.

REFERENCES

Balashov, S. P., E. S. Imasheva, T. G. Ebrey, B. N. Chen, D. R. Menick, and R. K. Crouch. 1997. Glutamate-194 to cysteine mutation inhibits fast light-induced proton release in bacteriorhodopsin. *Biochemistry.* 36:8671–8676.

Balashov, S. P., M. Lu, E. S. Imasheva, R. Govindjee, T. G. Ebrey, B. Othersen, III, Y. Chen, R. K. Crouch, and D. R. Menick. 1999. The proton release group of bacteriorhodopsin controls the rate of the final step of its photocycle at low pH. *Biochemistry.* 38:2026–2039.

Bogomolni, R. A., and J. L. Spudich. 1982. Identification of a third rhodopsin-like pigment in phototactic *Halobacterium halobium. Proc. Natl. Acad. Sci. USA.* 79:6250–6254.

Brown, L. S., J. Sasaki, H. Kandori, A. Maeda, R. Needleman, and J. K. Lanyi. 1995. Glutamic acid 204 is the terminal proton release group at the extracellular surface of bacteriorhodopsin. *J. Biol. Chem.* 270:27122–27126.

Brown, L. S., L. Bonet, R. Needleman, and J. K. Lanyi. 1993. Estimated acid dissociation constants of the Schiff base, Asp-85 and Arg-82, during the bacteriorhodopsin photocycle. *Biophys. J.* 65:124–130.

Chizhov, I., G. Schmies, R. Seidel, J. R. Sydor, B. Luttenberg, and M. Engelhard. 1998. The photophobic receptor from *Natronobacterium pharaonis*: temperature and pH dependencies of the photocycle of sensory rhodopsin II. *Biophys. J.* 75:999–1009.

Coutre, J., J. Tittor, D. Oesterhelt, and K. Gervert. 1995. Experimental evidence for hydrogen-bonded network proton-transfer in

bacteriorhodopsin shown by Fourier transform infrared spectroscopy using azide as catalyst. *Proc. Natl. Acad. Sci. USA.* 92:4962–4966.

Dioumaev, A. K., L. S. Brown, R. Needleman, and J. K. Lanyi. 1999. Fourier transform infrared spectra of a late intermediate of the bacteriorhodopsin photocycle suggest transient protonation of Asp-212. *Biochemistry.* 38:10070–10078.

Engelhard, M., B. Scharf, and F. Siebert. 1996. Protonation changes during the photocycle of sensory rhodopsin II from *Natronobacterium pharaonis*. *FEBS Lett.* 395:195–198.

Essen, L. O. 2002. Halorhodopsin: light-driven ion pumping made simple? *Curr. Opin. Struct. Biol.* 12:516–522.

Furutani, Y., M. Iwamoto, K. Shimono, N. Kamo, and H. Kandori. 2002. FTIR spectroscopy of the M-photointermediate in *pharaonis* phoborhodopsin. *Biophys. J.* 83:3482–3489.

Gordeliy, V. I., J. Labahn, R. Moukhametzianov, R. Efremov, J. Granzin, R. Schlesinger, G. Büldt, T. Savopol, A. J. Scheidig, J. P. Klare, and M. Engelhard. 2002. Molecular basis of transmembrane signalling by sensory rhodopsin II-transducer complex. *Nature.* 419:484–487.

Haupts, U., J. Tittor, and D. Oesterhelt. 1999. Closing in on bacteriorhodopsin: progress in understanding the molecule. *Annu. Rev. Biophys. Biomol. Struct.* 28:367–399.

Hessling, B., G. Souvignier, and K. Gerwert. 1993. A model-independent approach assigning bacteriorhodopsin's intramolecular reactions to photocycle intermediates. *Biophys. J.* 65:1929–1941.

Hirayama, J., Y. Imamoto, Y. Shichida, N. Kamo, H. Tomioka, and T. Yoshizawa. 1992. Photocycle of phoborhodopsin from haloalkaliphilic bacterium (*Natronobacterium pharaonis*) studied by low-temperature spectrophotometry. *Biochemistry.* 31:2093–2098.

Hoff, W. D., K. H. Jung, and J. L. Spudich. 1997. Molecular mechanism of photosignaling by archaeal sensory rhodopsins. *Annu. Rev. Biophys. Biomol. Struct.* 26:223–258.

Ikeura, Y., K. Shimono, M. Iwamoto, Y. Sudo, and N. Kamo. 2004. Role of Arg-82 of *pharaonis* phoborhodopsin (sensory rhodopsin II) on its photochemistry. *Biophys. J.* 86:3112–3120.

Iwamoto, M., Y. Furutani, Y. Sudo, K. Shimono, H. Kandori, and N. Kamo. 2002a. Role of Asp-193 in chromophore-protein interaction of *pharaonis* phoborhodopsin (sensory rhodopsin II). *Biophys. J.* 83:1130–1135.

Iwamoto, M., Y. Sudo, K. Shimono, and N. Kamo. 2002b. Illumination accelerates the decay of the O-intermediate of *pharaonis* phoborhodopsin (sensory rhodopsin II). *Photochem. Photobiol.* 76:462–466.

Iwamoto, M., Y. Furutani, N. Kamo, and H. Kandori. 2003a. Proton transfer reactions in the F86D and F86E mutants of *pharaonis* phoborhodopsin (sensory rhodopsin II). *Biochemistry.* 42:2790–2796.

Iwamoto, M., H. Kandori, and N. Kamo. 2003b. Photochemical properties of *pharaonis* phoborhodopsin (sensory rhodopsin II). *Recent Res. Dev. Chem.* 1:15–30.

Iwamoto, M., K. Shimono, M. Sumi, and N. Kamo. 1999. Positioning proton-donating residues to the Schiff-base accelerates the M-decay of *pharaonis* phoborhodopsin expressed in *Escherichia coli*. *Biophys. Chem.* 79:187–192.

Iwamoto, M., Y. Sudo, K. Shimono, and N. Kamo. 2001. Selective reaction of hydroxylamine with chromophore during the photocycle of *pharaonis* phoborhodopsin. *Biochim. Biophys. Acta.* 1514:152–158.

Iwamoto, M., C. Hasegawa, Y. Sudo, K. Shimono, T. Araiso, and N. Kamo. 2004. Proton release and uptake of *pharaonis* phoborhodopsin (sensory rhodopsin II) reconstituted into phospholipids. *Biochemistry.* 43:3195–3203.

Kandori, H., Y. Yamazaki, M. Hatanaka, R. Needleman, L. S. Brown, H. T. Richter, J. K. Lanyi, and A. Maeda. 1997. Time-resolved Fourier transform infrared study of structural changes in the last steps of the photocycle of Glu-204 and Leu-93 mutants of bacteriorhodopsin. *Biochemistry.* 36:5134–5141.

Kandori, H., K. Shimono, Y. Sudo, M. Iwamoto, Y. Shichida, and N. Kamo. 2001a. Structural changes of *pharaonis* phoborhodopsin upon photoisomerization of the retinal chromophore: infrared spectral comparison with bacteriorhodopsin. *Biochemistry.* 40:9238–9246.

Kandori, H., Y. Furutani, K. Shimono, Y. Shichida, and N. Kamo. 2001b. Internal water molecules of *pharaonis* phoborhodopsin studied by low-temperature infrared spectroscopy. *Biochemistry.* 40:15693–15698.

Klare, J. P., G. Schmies, I. Chizhov, K. Shimono, N. Kamo, and M. Engelhard. 2002. Probing the proton channel and the retinal binding site of *Natronobacterium pharaonis* sensory rhodopsin II. *Biophys. J.* 82:2156–2164.

Lanyi, J. K. 1993. Proton translocation mechanism and energetics in the light-driven pump bacteriorhodopsin. *Biochim. Biophys. Acta.* 1193:241–261.

Luecke, H., and J. K. Lanyi. 2003. Structural clues to the mechanism of ion pumping in bacteriorhodopsin. *Adv. Protein Chem.* 63:111–130.

Luecke, H., B. Schobert, J. K. Lanyi, E. N. Spudich, and J. L. Spudich. 2001. Crystal structure of sensory rhodopsin II at 2.4 Ångstroms: insights into color tuning and transducer interaction. *Science.* 293:1499–1503.

Matsuno-Yagi, A., and Y. Mukohata. 1977. Two possible roles of bacteriorhodopsin; a comparative study of strains of *Halobacterium halobium* differing in pigmentation. *Biochem. Biophys. Res. Commun.* 78:237–243.

Misra, S., R. Govindjee, T. G. Ebrey, N. Chen, J. X. Ma, and R. K. Crouch. 1997. Proton uptake and release are rate-limiting steps in the photocycle of the bacteriorhodopsin mutant E204Q. *Biochemistry.* 36:4875–4883.

Miyazaki, M., J. Hirayama, M. Hayakawa, and N. Kamo. 1992. Flash photolysis study on *pharaonis* phoborhodopsin from a haloalkaliphilic bacterium (*Natronobacterium pharaonis*). *Biochim. Biophys. Acta.* 1140: 22–29.

Oesterhelt, D., and W. Stoeckenius. 1971. Rhodopsin-like protein from the purple membrane of *Halobacterium halobium*. *Nat. New Biol.* 233:149–152.

Pebay-Peyroula, E., A. Royant, E. M. Landau, and J. Navarro. 2002. Structural basis for sensory rhodopsin function. *Biochim. Biophys. Acta.* 1565:196–205.

Richter, H. T., L. S. Brown, R. Needleman, and J. K. Lanyi. 1996. A linkage of the pK_a's of Asp-85 and Glu-204 forms part of the reprotonation switch of bacteriorhodopsin. *Biochemistry.* 35:4054–4062.

Royant, A., P. Nollert, K. Edman, R. Neutze, E. M. Landau, E. Pebay-Peyroula, and J. Navarro. 2001. X-ray structure of sensory rhodopsin II at 2.1-Å resolution. *Proc. Natl. Acad. Sci. USA.* 98:10131–10136.

Scharf, B., B. Pevec, B. Hess, and M. Engelhard. 1992. Biochemical and photochemical properties of the photophobic receptors from *Halobacterium halobium* and *Natronobacterium pharaonis*. *Eur. J. Biochem.* 206:359–366.

Schmies, G., B. Luttenberg, I. Chizhov, M. Engelhard, A. Becker, and E. Bamberg. 2000. Sensory rhodopsin II from the haloalkaliphilic *Natronobacterium pharaonis*: light-activated proton transfer reaction. *Biophys. J.* 78:967–976.

Seidel, R., B. Scharf, M. Gautel, K. Kleine, D. Oesterhelt, and M. Engelhard. 1995. The primary structure of sensory rhodopsin II: a member of an additional retinal protein subgroup is coexpressed with its transducer, the halobacterial transducer of rhodopsin II. *Proc. Natl. Acad. Sci. USA.* 92:3036–3040.

Shimono, K., M. Iwamoto, M. Sumi, and N. Kamo. 1997. Functional expression of *pharaonis* phoborhodopsin in *Escherichia coli*. *FEBS Lett.* 420:54–56.

Shimono, K., M. Kitami, M. Iwamoto, and N. Kamo. 2000. Involvement of two groups in reversal of the bathochromic shift of *pharaonis* phoborhodopsin by chloride at low pH. *Biophys. Chem.* 87:225–230.

Spudich, J. L., and H. Luecke. 2002. Sensory rhodopsin II: functional insights from structure. *Curr. Opin. Struct. Biol.* 12:540–546.

Sudo, Y., M. Iwamoto, K. Shimono, and N. Kamo. 2001a. *Pharaonis* phoborhodopsin binds to its cognate truncated transducer even in the presence of a detergent with a 1:1 stoichiometry. *Photochem. Photobiol.* 74:489–494.

Sudo, Y., M. Iwamoto, K. Shimono, M. Sumi, and N. Kamo. 2001b. Photoinduced proton transport of *pharaonis* phoborhodopsin (sensory rhodopsin II) is ceased by association with the transducer. *Biophys. J.* 80:916–922.

Takahashi, T., H. Tomioka, N. Kamo, and Y. Kobatake. 1985. A photosystem other than PS370 also mediates the negative phototaxis of *Halobacterium halobium*. *FEMS Microbiol. Lett.* 28:161–164.

Takao, K., T. Kikukawa, T. Asaiso, and N. Kamo. 1998. Azide accelerates the decay of M-intermediate of *pharaonis* phoborhodopsin. *Biophys. Chem.* 73:145–153.

Varo, G. 2000. Analogies between halorhodopsin and bacteriorhodopsin. *Biochim. Biophys. Acta.* 1460:220–229.

Wegener, A. A., I. Chizhov, M. Engelhard, and H. J. Steinhoff. 2000. Time-resolved detection of transient movement of helix F in spin-labelled *pharaonis* sensory rhodopsin II. *J. Mol. Biol.* 301:881–891.

Yan, B., T. Takahashi, R. Johnson, and J. L. Spudich. 1991. Identification of signaling states of a sensory receptor by modulation of lifetimes of stimulus-induced conformations: the case of sensory rhodopsin II. *Biochemistry.* 30:10686–10692.